Conference Proceedings

Solar World Congress 2015
Daegu, Korea, 08 – 12 November 2015

Novel Encapsulation Technique to Upscale Latent Heat Storage Capacity in Steam Accumulators

Hakeem Niyas, P. Muthukumar

Department of Mechanical Engineering, Indian Institute of Technology Guwahati, Assam, India

Abstract

Cylindrical latent heat storage (LHS) capsules are used in steam accumulators for reducing the pressure drop in the vessel. Due to the high thermal resistance offered by the phase change material (PCM) in capsules with a higher diameter, more number of less diameter capsules need to be used for a particular storage capacity. In the present study, a novel encapsulation technique is proposed for effective heat transfer in cylindrical LHS capsules. With this technique, less number of capsules can yield the similar or higher storage capacity in a comparatively lesser charging time. A numerical model is developed to study the performance characteristics of the proposed novel encapsulation technique. In the numerical model, the effective heat capacity method is applied to consider the latent heat of the PCM and Boussinesq approximation is used to include the natural convection of the molten layer of the PCM. Darcy law's source term is added in the momentum equation to deduce the velocities of the PCM in its actual form in the mushy zone.

Keywords: *Heat transfer enhancement, Latent heat storage, Novel encapsulation, Phase change material.*

1. Introduction

Steam accumulators are applied as buffer storage devices between steam generators and consumers in case of a mismatch between the steam production and consumption (Stevanovic et al., 2012). During discharge in a steam accumulator, the steam pressure drops. Two viable techniques such as incorporating a flash evaporator or an encapsulated latent heat storage (LHS) capsule are preferred to avoid the pressure drop. Due to the exergy loss by mixing in the flash evaporator system, encapsulated LHS capsule is advantageous (Steinmann and Eck, 2006). Cylindrical capsules were being used normally in commercial steam accumulators (Medrano et al., 2010). Several experimental and numerical studies were carried out to study the LHS characteristics of cylindrical capsules during both charging and discharging processes (Bourdillon et al., 2015; Himeno et al., 1988; Steinmann and Tamme, 2008). Certain reviews encompass the major research works on encapsulated systems (Farid et al., 2004; Su et al., 2015). Despite of several advantages like reduction of temperature transients in steam accumulator, high volume-specific storage capacity, etc. (Medrano et al., 2010), the major disadvantage of encapsulated LHS capsule is the limitation in the diameter of the cylindrical capsules. With an increase of diameter, the resistance to heat transfer also increases due to the low thermal conductivity of the phase change material (PCM). In the present study, a novel encapsulation technique is proposed to alleviate this. The novelty proposed here is to use a shell-and-tube LHS system with a very small inner tube. With this, the heat transfer would be enhanced due to lesser thickness of PCM and increased heat transfer area when compared to the LHS capsule having basic encapsulation. For comparing the performance characteristics of the basic and proposed novel technique, capsules having a LHS capacity of 0.25 MJ are considered. Sodium nitrate and SS304 are selected as the PCM and encapsulating material. The thermo-physical properties of sodium nitrate are given in Tab. 1. Figure 1 shows the schematic of the cylindrical capsule and novel encapsulated cylindrical capsule. The diameter of the LHS capsules having basic and novel encapsulation for storing the corresponding LHS capacity are 63.5 mm and 64.3 mm. A small tube of diameter 6 mm is used as the inner tube for the novel capsule. The design of capsules is made in such a way that the volume of PCM in both the capsules are same.

doi:10.18086/swc.2015.02.17 Available at http://proceedings.ises.org

Tab. 1: Thermo-physical properties of sodium nitrate

Properties	Values	References
Density (ρ, kg m^{-3})		Bauer et al., 2012
Solid phase	2130	
Mushy zone	Linear interpolation	
Liquid phase	1908	
Latent heat of fusion (ΔH_f, J kg^{-1})	178,000	
Dynamic viscosity (μ, Pa s)	$0.0119 - 1.53 \times 10^{-5}\ T$	Janz et al., 1979
Melting point (T_m, K)	579.95	
Specific heat (c, J kg^{-1} K^{-1})	$444.53 + 2.18\ T$	Lan and Kou, 1991
Thermal expansion coefficient (β, K^{-1})	6.6×10^{-4}	
Thermal conductivity (k, W m^{-1} K^{-1})	$0.3057 + 4.47 \times 10^{-4}\ T$	White and Davis, 1967

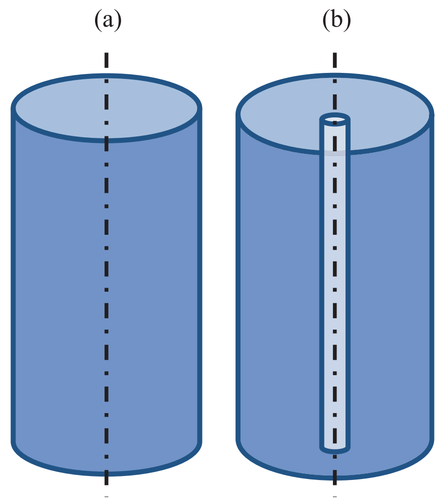

Fig. 1: Schematic diagram of encapsulated capsules (a) basic (b) novel

2. Numerical model

Three physical processes are to be simulated to study the LHS behavior of encapsulated LHS capsules, i.e. conduction, phase change and convection. A 2-D axisymmetric model is developed in view of the symmetry of flow and heat transfer around the vertical axis. Molten PCM movement due to natural convection heat transfer within the capsules is assumed to be laminar, Newtonian and incompressible. The major difficulty in the modeling of LHS system is the inclusion of latent heat and this is implemented using effective heat capacity method wherein a single term called effective heat capacity is used to consider both sensible and latent heat. The simulation is modelled using COMSOL Multiphysics software and the discontinuous effective heat capacity is applied using a Heaviside function. Buoyancy effect of the molten PCM is incorporated using Boussinesq approximation. To properly interpret the velocities in mushy zone, Darcy law's source term is added in the momentum equation. The governing equations and their corresponding sub-equations are given in Eqs. (1-8). Capsules are initially kept at 564.95 K and 594.95 K during charging and discharging processes. At any time ($t > 0$), the boundaries are given a temperature of 594.95 K and 564.95 K during charging and discharging processes thereby making a temperature swing of 30 K. The major performance parameter used in LHS is melt fraction. Melt fraction of the PCM can be calculated based on the lever rule applied between the solidus and liquidus temperatures and it is given by Eq. (8). During charging / discharging, melt fraction of the PCM possess a value of 0 / 1 initially and when it reaches a value of 1 / 0, it is said to be completely charged / discharged.

$$c = \begin{cases} c_{ps} & for\ T < T_S \\ c_{p,eff} & for\ T_S \le T \le T_L \\ c_{pl} & for\ T > T_L \end{cases} \quad \text{(Eq. 1)}$$

$$c_{p,eff} = \frac{c_{ps} + c_{pl}}{2} + \frac{\Delta H_f}{2\Delta T_m} \quad \text{(Eq. 2)}$$

$$\nabla . \vec{V} = 0 \quad \text{(Eq. 3)}$$

$$\frac{\partial \vec{V}}{\partial t} + (\vec{V}.\nabla)\vec{V} = \frac{1}{\rho}\left(-\nabla P + \mu \nabla^2 \vec{V} + F + \vec{S}\right) \quad \text{(Eq. 4)}$$

$$\rho c \frac{DT}{Dt} = k \nabla^2 T \quad \text{(Eq. 5)}$$

$$F = \rho \vec{g} \beta \left(T - T_m\right) \quad \text{(Eq. 6)}$$

$$\vec{S} = \frac{\left(1-\theta\right)^2}{(\theta^3 + \varepsilon)} A_{mush} \vec{V} \quad \text{(Eq. 7)}$$

$$\theta = \frac{T - T_S}{T_L - T_S} = \frac{T - T_m + \Delta T_m}{2\Delta T_m} = \begin{cases} 0 & for\ T < T_S \\ 0-1 & for\ T_S \le T \le T_L \\ 1 & for\ T > T_L \end{cases} \quad \text{(Eq. 8)}$$

3. Results and discussions

3.1. Grid Independency Test

Free triangular mesh is adapted in the developed numerical model. In order to test the dependency of numerical results on the mesh element size, a simulation is ran with the novel cylindrical capsule for charging process. The LHS capsule is initially at 564.95 K. At any time t > 0, the boundaries of the capsule are given 594.95 K. The average temperature of the capsule is compared for different element sizes viz. 10408, 12031 and 14410 elements. It is observed from Fig. 2 that the model with 12031 elements is found to be grid independent. Similarly, grid independency test carried out for the basic cylindrical capsule yields an optimum mesh size with 11672 elements.

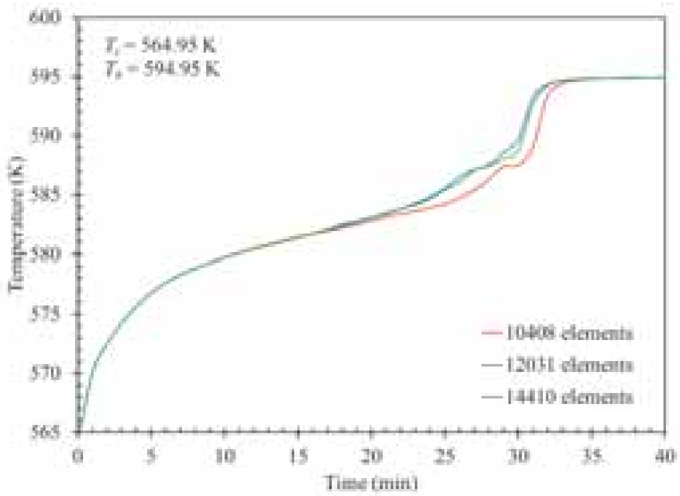

Fig. 2: Grid independent test

3.2. Temperature Distribution – Charging

Figure. 3 shows the comparison of the average temperature variation of the basic and novel LHS capsules during charging process. PCM kept in the capsules during charging is initially in the solid state at 564.95 K. When an uniform high temperature of 594.95 K is given on the boundary of the capsule, heat is transferred from periphery of the capsules and stored in the form of sensible and latent heat. It is inferred from Fig. 3 that the increase in average temperature is faster in LHS capsule having novel encapsulation than basic encapsulation. This is due to 2 reasons viz., increased surface area available for heat transfer and reduced thickness of the PCM layer.

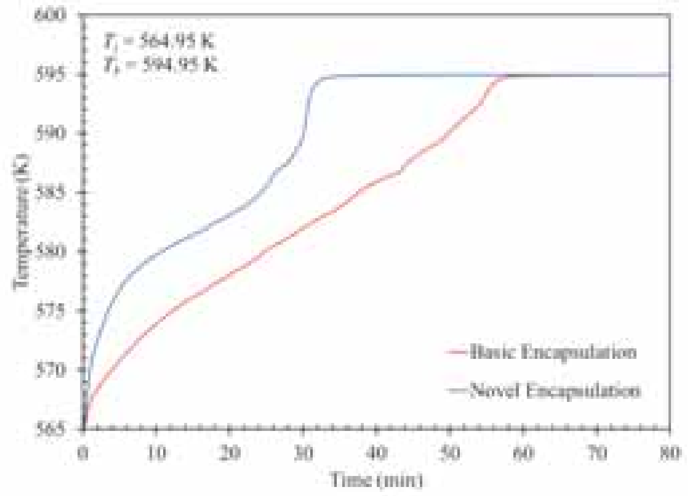

Fig. 3: Temperature distribution during charging

3.3. Charging Time

Charging time of the LHS capsule is defined with respect to the melt fraction of the PCM. The LHS capsule is said to be fully charged when the melt fraction of the PCM reaches unity. Figure. 4 shows the comparison of average melt fraction variation of basic and novel LHS capsules. It can be noted from Fig. 4 that the charging time of novel capsules is lesser than the basic capsule. It takes about 57 min and 32 min for complete charging of the PCM in LHS capsules having basic and novel encapsulation. There is a charging time reduction of 44 % in capsule having novel encapsulation when compared with the basic encapsulation. Screenshots of melt fraction variation of LHS capsules during charging are given in Fig. 5. The effect of natural convective heat transfer can be seen from the asymmetric temperature variation in the capsules at 15, 30, 45 min (basic encapsulation) and 30 min (novel encapsulation).

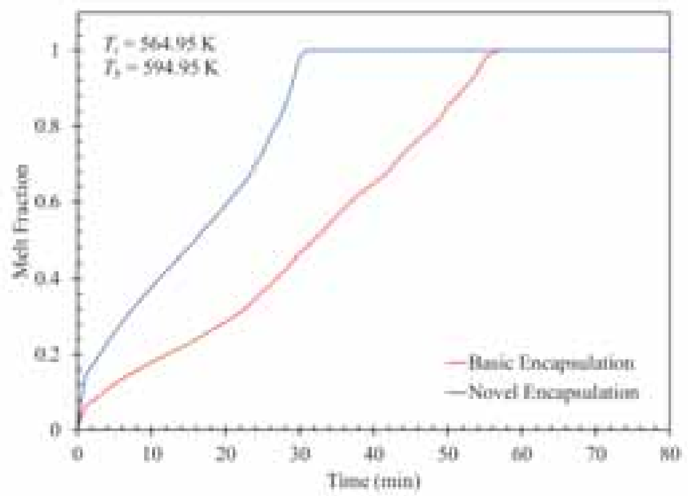

Fig. 4: Melt fraction distribution during charging

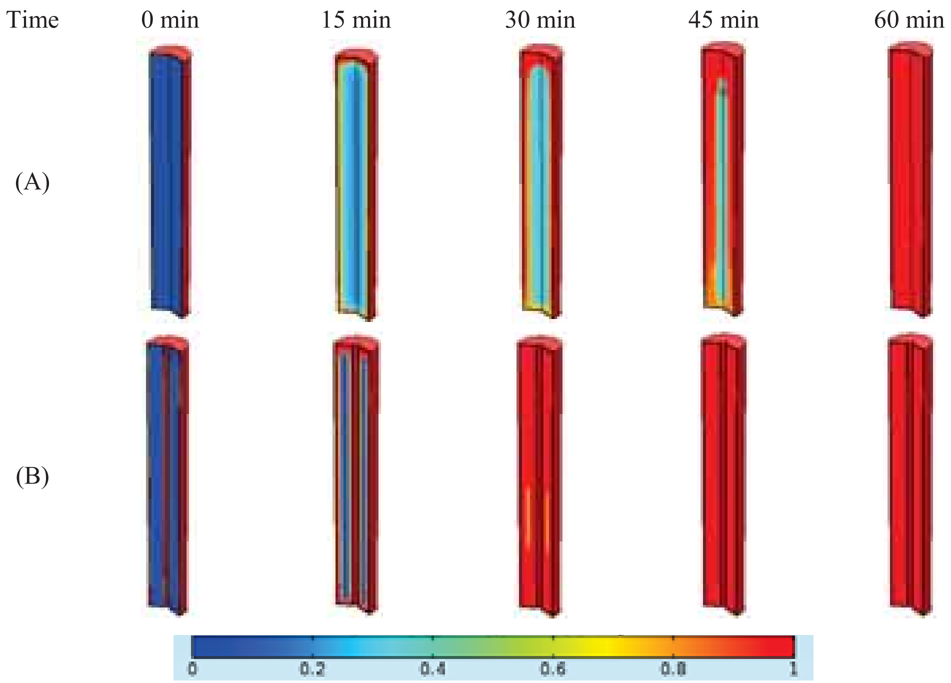

Fig. 5: Melt fraction distribution during charging (A) Basic encapsulation (B) Novel encapsulation

3.4. Temperature Distribution – Discharging

Figure. 6 shows the comparison of the average temperature variation of the LHS capsules having basic and novel encapsulation during discharging process. PCM kept in the capsules during discharging is initially in the liquid state at 594.95 K. When an uniform low temperature of 564.95 K is given on the boundary of the capsule, heat is transferred from the capsules and gets discharged in the form of sensible and latent heat. It is inferred from Fig. 6 that the decrease in average temperature is faster in LHS capsule having novel encapsulation than the basic encapsulation similar to the charging process.

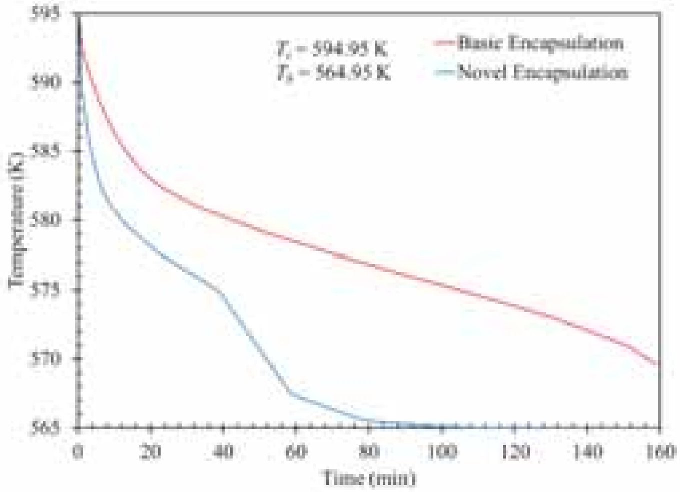

Fig. 6: Temperature distribution during discharging

3.5. Discharging Time

Discharging time of the LHS capsule is defined similarly with respect to the melt fraction of the PCM. The LHS capsule is said to be fully discharged when the melt fraction of the PCM reaches zero. Figure. 7 shows the comparison of average melt fraction variation LHS capsules having basic and novel encapsulation. It can be noted from Fig. 7 that the discharging time of novel capsules is much lesser than the basic capsule. It takes about 158 min and 48 min for complete discharging of the PCM in LHS capsules having basic and novel encapsulation. There is a discharging time reduction of 70 % in capsule having novel encapsulation when compared with the basic encapsulation. Screenshots of melt fraction variation of LHS capsules during discharging are given in Fig. 8. It can be understood from Fig. 8 that solidification of PCM is highly dominated by conductive heat transfer and less or no influence by natural convection heat transfer.

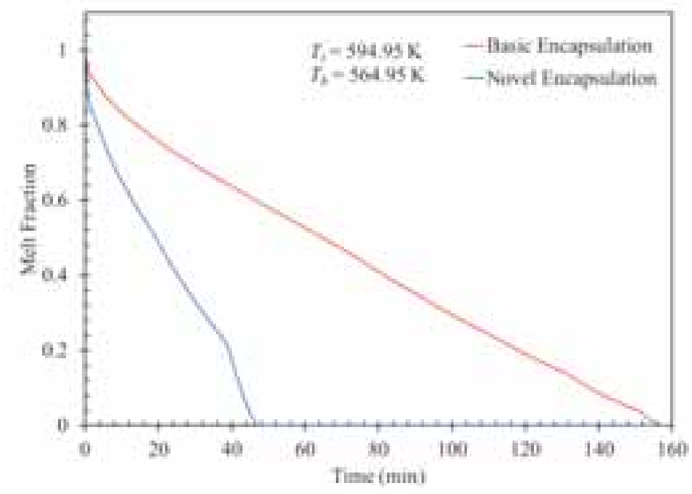

Fig. 7: Melt fraction distribution during charging

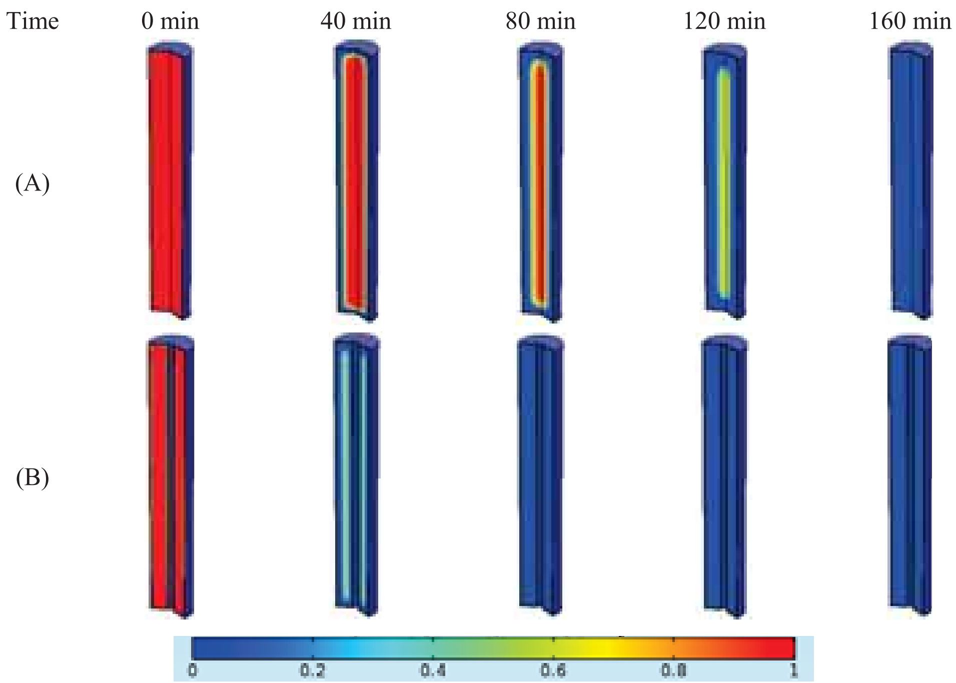

Fig. 8: Melt fraction distribution during charging

4. Conclusions

A thermal model was developed to compare the performance of LHS capsules having basic and novel encapsulation during charging and discharging processes. It was found that the charging of PCMs in both the models was dominated by natural convection. Numerical results shown that for the same mass of PCM, LHS capsules with novel encapsulation yields lesser charging and discharging time than the capsule with basic encapsulation. This is due to 2 reasons viz., increased surface area available for heat transfer and reduced thickness of the PCM layer. It took about 57 min and 32 min for complete charging and 158 min and 48 min for complete discharging in the LHS capsules with basic and novel encapsulation. It can be noted that the charging and discharging time of the LHS capsule with novel encapsulation shown a reduction of about 44 % and 70 % respectively when compared with the LHS capsule with basic encapsulation. The results of the current study will be useful in the design of compact and efficient LHS encapsulated capsules.

5. Acknowledgements

The authors sincerely thank the Department of Science and Technology (DST), Government of India, for their financial support (Project No: DST/TM/SERI/2K10/53(G)).

6. References

Bauer, T., Laing, D., Tamme, R., 2012. Characterization of sodium nitrate as phase change material. Int. J. Thermphys. 33, 91-104.

Bourdillon, A.C., Verdin, P.G., Thompson, C.P., 2015. Numerical simulations of water freezing processes in cavities and cylindrical enclosures. Appl. Therm. Eng. 75, 839-855.

Farid, M.M., Khudhair, A.M., Razack, S.A.K., Al-Hallaj, S., 2004. A review on phase change energy storage: materials and applications. Energy Convers. Manage. 45, 1597-1615.

Himeno, N., Hijikata, K., Sekikawa, A., 1988. Latent heat thermal energy storage of a binary mixture-flow and heat transfer characteristics in a horizontal cylinder. Int. J. Heat Mass Transfer. 31 (2), 359-366.

Janz, G.J., Allen, C.B., Bansal, N.P., Murphy, R.M., Tomkins, R.P.T., 1979. Physical Properties Data Compilations Relevant to Energy Storage. II. Molten Salts: Data on Single and Multi-component Salt Systems, NSRDS-NBS-61 (Pt. 2), U.S. National Bureau of Standards. <http://www.nist.gov/data/nsrds/NSRDS-NBS61-II.pdf> (Last accessed 01.11.2015)

Lan, C.W., Kou, S., 1991. Effects of rotation on heat transfer, fluid flow and interfaces in normal gravity floating-zone crystal growth. J. Cryst. Growth. 114, 517-535.

Medrano, M., Gil, A., Martorell, I., Potau, X., Cabeza, L.F., 2010. State of the art on high-temperature thermal energy storage for power generation. Part 2—Case studies. Renewable Sustainable Energy Rev. 14, 56-72.

Steinmann, W.D., Eck, M., 2006. Buffer storage for direct steam generation, Sol. Energy. 80, 1277-1282.

Steinmann, W.D., Tamme, R., 2008. Latent heat storage for solar steam systems. J. Sol. Energy Eng. 130, 011004:1–5.

Stevanovic, V.D., Maslovaric, B., Prica, S., 2012. Dynamics of steam accumulation. Appl. Therm. Eng. 37, 73–79.

Su, W., Darkwa, J., Kokogiannakis, G., 2015. Review of solid–liquid phase change materials and their encapsulation technologies. Renewable Sustainable Energy Rev. 48, 373-391.

White, L.R., Davis, H.T., 1967. Thermal conductivity of molten alkali nitrates. J. Chem. Phys. 47, 5433-5439.